ADVANCES IN ATMOSPHERIC SCIENCES, VOL. 38, MARCH 2021, 413–429

• **Original Paper** •

Sensitivity of Snowfall Characteristics to Meteorological Conditions in the Yeongdong Region of Korea

Yoo-Jun KIM*[1], So-Ra IN[2], Hae-Min KIM[1], Jin-Hwa LEE[1], Kyu Rang KIM[1], Seungbum KIM[1], and Byung-Gon KIM[3]

[1]*High Impact Weather Research Department*, *National Institute of Meteorological Sciences*, *Gangneung* 25457, *Korea*

[2]*Operational Systems Development Department*, *National Institute of Meteorological Sciences*, *Seogwipo* 63568, *Korea*

[3]*Department of Atmospheric Environmental Sciences*, *Gangneung-Wonju National University*, *Gangneung* 25457, *Korea*

(Received 28 May 2020; revised 18 September 2020; accepted 13 October 2020)

ABSTRACT

This study investigates the characteristics of cold clouds and snowfall in both the Yeongdong coastal and mountainous regions under different meteorological conditions based on the integration of numerical modeling and three-hourly rawinsonde observations with snow crystal photographs for a snowfall event that occurred on 29–30 January 2016. We found that rimed particles predominantly observed turned into dendrite particles in the latter period of the episode when the 850 hPa temperature decreased at the coastal site, whereas the snow crystal habits at the mountainous site were largely needle or rimed needle. Rawinsonde soundings showed a well-defined, two-layered cloud structure along with distinctive wind-directional shear, and an inversion in the equivalent potential temperature above the low-level cloud layer. The first experiment with a decrease in lower-layer temperature showed that the low-level cloud thickness was reduced to less than 1.5 km, and the accumulated precipitation was decreased by 87% compared with the control experiment. The difference in precipitation amount between the single-layered experiment and control experiment (two-layered) was not so significant to attribute it to the effect of the seeder–feeder mechanism. The precipitation in the last experiment by weakening wind-directional shear was increased by 1.4 times greater than the control experiment specifically at the coastal site, with graupel particles accounting for the highest proportion (~62%). The current results would improve snowfall forecasts in complicated geographical environments such as Yeongdong in terms of snow crystal habit as well as snowfall amount in both time and space domains.

Key words: Yeongdong, snow crystal, rawinsonde, cloud-resolving model

Citation: Kim, Y.-J., S.-R. In, H.-M. Kim, J.-H. Lee, K.-R. Kim, S. Kim, and B.-G. Kim, 2021: Sensitivity of snowfall characteristics to meteorological conditions in the Yeongdong region of Korea. *Adv. Atmos. Sci.*, **38**(3), 413–429, https://doi.org/10.1007/s00376-020-0157-9.

Article Highlights:

- Two-layered cold cloud and snowfall were well represented by a cloud-resolving model.
- Sensitivity experiments with decreased temperature showed a decrease in rainfall and increase in graupel and snow.
- The simulation with weakening of wind-directional shear led to vertical cloud invigoration and significant change in snowfall.

1. Introduction

One of the most challenging topics of winter weather forecasting is to determine the occurrence and phase of precipitation on and around complex mountainous areas (Thériault et al., 2012). The Yeongdong region of the Korean Peninsula is characterized by frequent snowfall in winter due to its complex orographic features and the East Sea effect (Nam et al., 2014; Kim et al., 2018). It is even amplified by the nearby (⩽ 10 km) Taebaek mountain range with an average altitude of 1000 m to the west and the relatively warmer East Sea to the east. The East Sea effect on snow is similar to the lake effect on snow in terms of genesis. As the cold air passes over the relatively warm East Sea, heat and moisture are transferred into the lower atmosphere. According to the Statistical Yearbook of Natural Disasters (Ministry of the Interior and Safety, 2016), 24% of the damage caused by heavy snowfall over the past 10 years has been concentrated in the Yeongdong region, representing the largest pro-

* Corresponding author: Yoo-Jun KIM
Email: yoojun@korea.kr

portion among the 16 provinces in South Korea. Heavy snowfall is a typical meteorological disaster in winter in this region, occurring three times as often as in the Yeongseo region on the western side of the Taebaek mountain range. However, winter snowfall forecasting is extremely difficult in the Yeongdong region due to the interaction between complex orographic and oceanic features (Kwon et al., 2006).

On the other hand, numerical simulations have demonstrated that snowfall intensity and location can vary depending on the snow crystal type (Lin et al., 2011). The microphysical characteristics of snow crystals are important in forecasting snowfall events as well as remote sensing, such as satellite and radar, because they determine the scattering and absorption properties of snow crystals (Liu, 2008; Molthan et al., 2010; Cooper et al., 2017). In particular, ice-phase particles have different shapes and sizes, which make theoretical studies on ice-phase particles more challenging compared with studies on liquid water particles, and further lead to uncertainties in cloud modeling.

Snow crystals grow through the processes of riming and aggregation when supercooled liquid drops freeze directly onto ice-phase particles or causes them to stick together. Riming and aggregation tend to produce rapidly precipitating particles by enhancing precipitation on the leeward side of a mountain range (Medina and Houze, 2015). Ice-phase particles can also grow while they fall into lower-level frontal clouds by the "seeder–feeder" mechanism, as hypothetically proposed by Bergeron (1950). Houze et al. (1981) highlighted the role of mesoscale upstream motions in condensing cloud water for the ice-phase particles formed in the upper-level cloud to aggregate as they fall through the lower-level cloud.

The seeder–feeder process frequently occurs over and near complex mountainous terrain and plays an important role in precipitation formation and enhancement. Extensive research based on dual polarimetric radar observations has been conducted worldwide to understand the microphysical processes of snow crystals, such as riming and aggregation (Schneebeli et al., 2013; Grazioli et al., 2015; Oue et al., 2016). Despite this research trend, however, only a very limited number of observational and modeling studies have been conducted to investigate snow crystal characteristics in the Korean Peninsula. Seo et al. (2015) presented snowfall and snow crystal characteristics using a digital camera mounted with a magnifier and a rawinsonde during the 2014 Experiment of Snow Storms At Yeongdong (ESSAY) campaign. Kim et al. (2018) conducted intensive observations and modeling-based analysis and showed how snow crystals change from riming to aggregate type during snowfall episodes, be it from a single-layered or two-layered cloud structure, as the 850 hPa temperature decreases.

In this regard, Houze and Medina (2005) and Medina and Houze (2015) presented a conceptual model for atmospheric dynamics and microphysical mechanisms associated with the topographic enhancement of precipitation. They showed that meteorological conditions can have great impacts on snow crystal characteristics; for example, upstream flow can induce precipitation enhancement through coalescence and riming, and aggregation due to the differences in the fall speeds among ice particles. The Yeongdong region is also subject to strong orographic effects along with the East Sea effect. Although great efforts have been made to elucidate snowfall mechanisms and improve forecasting accuracy using a variety of data and analysis methods, a lack of ground-based, remote-profiling, and aircraft in-situ measurements has hindered efforts to improve precipitation forecast accuracy in the Yeongdong region. Furthermore, the constraints of dual-polarization radars, such as the beam blockage issues in mountainous regions, heat release problems, and complicated assumptions (WMO, 2008; Maahn and Kollias, 2012; Schneebeli et al., 2013), limit the available insight into the complicated microphysical processes in mixed-phase clouds in the complex terrain (Grazioli et al., 2015).

To bridge this research gap and overcome the limitations of previous radar-based studies, this study aims to integrate intensive (3-h interval) rawinsonde observations and cloud-resolving model output to provide an in-depth understanding of winter snowfall in the Yeongdong region and shed light on the evolution of snow crystal characteristics in response to varying meteorological characteristics. Additionally, using a cloud-resolving model, we seek to identify the effects of major meteorological factors on snowfall and snow crystal characteristics specific to the Yeongdong region, which remained yet unexplained in Kim et al. (2018). To this end, we selected a heavy snowfall episode that occurred on 29–30 January 2016, during which intensive observations were undertaken in both the Yeongdong coastal and mountainous regions, including rawinsonde observations with high temporal resolution (3-h) and snowflake photography, and we present the results of numerical simulation sensitivity experiments, in which realistic meteorological characteristics such as temperature, seeder–feeder structure, and wind-directional shear critical for snowfall in this region can be reflected.

2. Data and methods

The ESSAY campaign has been carried out since 2013 to understand the characteristics of winter snowfall in the Yeongdong region. We used three-hourly rawinsonde data and snowflake photographs obtained during the ESSAY-2016 campaign to gain insight into the cold cloud and snow crystal characteristics in the Yeongdong region under various meteorological conditions. We focus on the Gangneung-Wonju National University (GWNU) and Daegwallyeong (DAGW) sites as coastal and mountainous regions, respectively (Fig. 1). We also investigated precipitation characteristics using data from the Automated Surface Observing System and Automatic Weather Station at Bukgangneung and Daegwallyeong stations, respectively (Table 1). Precipitation amounts are usually measured every

hour with weighing precipitation gauges with automatic drains, and snowfall amounts are manually measured every three hours using snow plate and closed-circuit television (CCTV), respectively. In addition, radar reflectivity, fall velocity and liquid water content are obtained from micro rain radar (MRR) measurements at Alpensia (ALPN) site. The mean diameter and number concentration of droplets are also determined by a PARSIVEL disdrometer at the same site (Table 1).

For snow crystal observations, we used both a smartphone and digital camera mounted with 20× and 5× magnifiers, respectively. Since the resolution of snow crystals photographed by the smartphone is better than digital camera, photos taken with the smartphone camera were mostly used for determining the snow crystal type. To keep the shape of the snow crystals falling on the snow plate as intact as possible, we used a soft black fleece cloth and stored the observation plate outside to prevent snow crystals from melting. A detailed description of the snow crystal observation method can be found in Seo et al. (2015). The same method has been used in other countries, such as at the Science of Nowcasting Olympic Weather for Vancouver 2010 (SNOW-V10) campaign (Thériault et al., 2012, 2014). Unlike conventional remote sensing–based snow crystal observations, these observed data are also expected to help us better understand snowfall events. We also try to analyze the changes of main snow crystals and 850 hPa temperature with time. Here, we assume 850 hPa as the altitude where the snow crystals are formed because the mean height of cold clouds in the Yeongdong region was observed to be about 1–2 km above sea level (Seo et al., 2015; Ko et al., 2016).

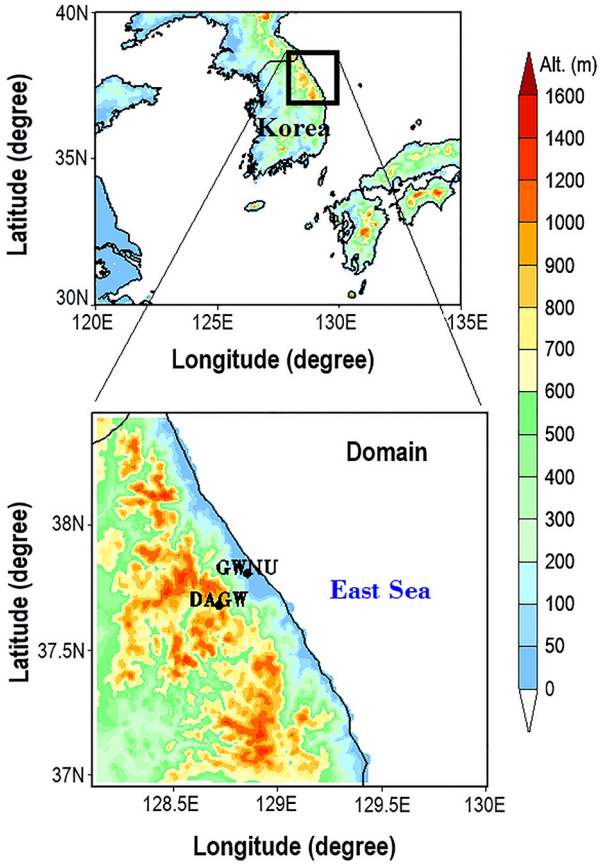

Fig. 1. Model domain and topography [adapted from Kim et al. (2018)].

Additionally, we used the Cloud Resolving Storm Simulator (CReSS) model to simulate the observed snow cloud systems and snow crystal characteristics. The CReSS model is a three-dimensional, non-hydrostatic model developed by the Hydrospheric Atmospheric Research Center of Nagoya University, Japan; it was designed to realistically simulate mesoscale systems (Tsuboki and Sakakibara, 2001). To gain an in-depth understanding of the effects of meteorological conditions on snow crystal characteristics in the Yeongdong region, we selected a heavy snowfall episode that occurred on 29–30 January 2016 during the ESSAY campaign period. We performed sensitivity experiments using the CReSS model. The snowfall episode selected is a two-layered cloud system associated with low pressure passing through the region, which allows for a variety of sensitivity designs with changing meteorological conditions.

As initial and boundary conditions for the numerical simulation, we used the mesoscale model (MSM) analysis data provided by the Japan Meteorological Agency (JMA). It has 5-km horizontal resolution, 16 isobaric planes, and an integration period of 30 h (Table 2). For the cloud microphysical process, we used a bulk cold rain scheme and selected the 1.5-order turbulence kinetic energy closure scheme for sub-

Table 1. Observational variables and instruments used in this study.

Variables (Intervals)	Instruments (Site)	Manufacturer (Model)
Vertical profile (3-h or 6-h)	Rawinsonde (GWNU & DAGW)	GRAW (DFM-09)
Snow crystals (3-h)	Smartphone & Digital camera (GWNU & DAGW)	Apple (iPhone 5) & Canon (EOS 650D)
Snowfall amounts (3-h)	Snow measuring plate & CCTV (Bukgangneung & Daegwallyeong Station)	–
Precipitation amounts (1-h)	Auto-emptying type weighing precipitation gauge (Bukgangneung & Daegwallyeong Station)	Wellbian system (WPG-A1)
Radar reflectivity, Fall velocity and Liquid water content (1-min)	Micro rain radar (ALPN[a])	METEK (MRR-2)
Mean diameter and number concentration of droplet (1-min)	PARSIVEL disdrometer (ALPN[a])	OTT (PARSIVEL-2)

Note: ALPN[a] (852 m above the sea level) denotes a supersite located within 4 km of the DAGW site.

Table 2. Summary of the CReSS (Version 3.5.0) model setup used in this study.

Model parameters	Setup
Integration period	0000 UTC 29 January 2016 to 0600 UTC 30 January 2016
Initial and lateral boundary conditions	JMA-MSM Analysis: 481 × 505 (5 km)
Microphysics	Bulk cold rain scheme
Planetary boundary layer parameterization	1.5-order turbulent closure scheme
Grid size	Horizontal: 1 km / Vertical: 200 m
Dimension	Horizontal: 160 × 160 / Vertical: 50 layers
Temporal interval	30-min

grid-scale parameterization (Tsuboki and Sakakibara, 2002). The microphysical processes in the CReSS model include three basic categories of processes in the liquid and ice phases: phase nucleation, growth or evaporation by diffusion, and inter-particle collection (Murakami, 1990; Murakami et al., 1994; Lee et al., 2010). In the CReSS model, surface precipitation is classified into three types such as rain, graupel, and snow, depending on the density and fall velocity of particles (Tsuboki and Sakakibara, 2007). The domain of the CReSS model configured in this study has a resolution of 1000 m (horizontal) × 200 m (vertical) in the Yeongdong region, as illustrated in Fig. 1. The detailed model design and configuration options are outlined in Table 2.

For sensitivity tests, the JMA-MSM data, which are used as the initial and boundary conditions, need to be corrected or modified. The JMA-MSM binary file information indicates that there are 13 variables and 17 vertical layers, including the surface layer. Of the initial and boundary conditions used in the control (CTRL) experiment, we changed the air temperature, relative humidity (RH), and the wind components (u and v). We modified the background field for the sensitivity experiments. First, the initial data for the temperature reduction (TEMP) experiment were generated by cooling the low-level ($\leqslant$ 850 hPa of the CTRL experimental background conditions) temperature by 3°C in comparison with the CTRL (Figs. 2a and 2b) to evaluate the dependency of temperature in precipitation particle characteristics below the 850 hPa altitude, one of the most remarkable characteristics of the snowfall events in the Yeongdong region (Kim et al., 2018). Secondly, in order to investigate the effects of the seeder–feeder mechanisms on snowfall in this region, the background field for single-layered cloud (CLOD) experiment was modified by lowering the RH values between 700 hPa and 300 hPa to 30%, as illustrated in Fig. 2d.

Lastly, we generated the initial data for the wind shear weakening (WIND) experiment to investigate the effect of wind-directional shear above the cloud layer. We changed the wind direction at a given altitude using a simple u and v conversion formula. As illustrated in Fig. 2f, the wind field in the vicinity of the shear layer was smoothed by naturally weakening the wind direction to the Ekman spiral shape at an altitude between 850 hPa and 600 hPa, and to the same as in the CTRL experiment at altitudes above 500 hPa in order to preserve the upper-level dynamics. By performing various sensitivity experiments based on the local meteorological characteristics of the Yeongdong region, such as orographic (Taebaek mountain) and oceanic (East Sea) effects, our intention was to investigate the snowfall and snow crystal characteristics that vary under the influence of the two-layered cloud structure, 850-hPa temperature, and wind-directional shear.

3. Results

3.1. *Synoptic-scale meteorological characteristics*

To investigate the effects of meteorological conditions on snow crystal characteristics, we selected a heavy snowfall episode that occurred on 29–30 January 2016: a synoptic-scale, low-pressure system that was passing through the region (Ko et al., 2016). Such events are frequently observed in the Yeongdong region and thus allow for a variety of sensitivity designs with changing meteorological conditions. Figure 3a shows the surface weather chart for 1200 UTC 29 January 2016. The Siberian high extending to the East Sea and the low pressure over southeastern Japan provide favorable synoptic conditions for bringing northeasterly wind to the Yeongdong region. Moreover, the upper-level (500 hPa) synoptic chart verifies the presence of a cold low and a mesoscale thermal trough over the Korean Peninsula along with an isobaric line with east–west orientation (Fig. 3b). In the 500 hPa chart in Fig. 3b, a −30°C isothermal line (red solid line) is drawn over the northern part of the Korean Peninsula. This synoptic condition favors an easterly-induced cloud system, leading to precipitation enhancement along the east coast of the Korean Peninsula (Fig. 4a).

Then, we compared the radial velocity characteristics of the upper and lower cloud layers observed via the S-band Doppler radar currently operating in Gangneung to identify cloud structures associated with the snowfall event (Figs. 3c and d). The green (+) radial velocity signal is the wind coming towards the radar antenna, and the yellow (−) signal indicates the wind moving away from the radar antenna. Analysis revealed distinct differences in the radial velocity between the upper level (3 km) and lower level (1 km). At a 3-km altitude, westerly wind was predominant in the Yeongdong region (Fig. 3c), whereas at a 1-km altitude northeasterly wind was remarkable (Fig. 3d), as identified by the

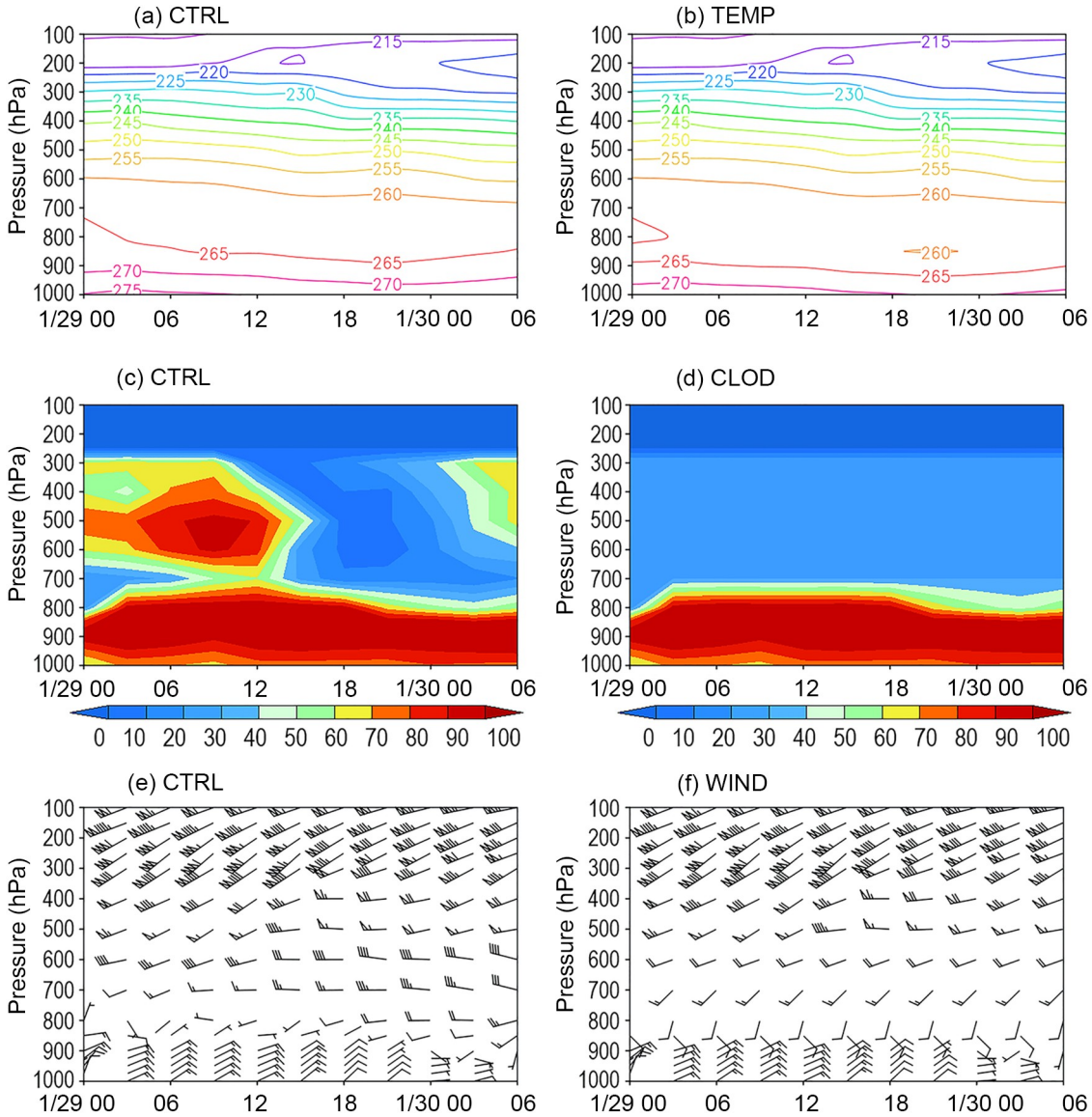

Fig. 2. Time–height distributions of temperature (contours; units: K), relative humidity (color shading; units: %), and wind field (wind barbs; units: m s^{-1}) from 0000 UTC 29 January 2016 to 0600 UTC 30 January 2016 for the control (CTRL) and sensitivity experiments (TEMP, CLOD, and WIND) using the mesoscale model (MSM).

radial velocity signals. This means that the westerly and easterly-induced cloud systems were moving in opposite directions at the upper and lower cloud layers, respectively.

3.2. *Atmospheric structure and snow crystal characteristics*

3.2.1. *Coastal site*

We used three-hourly rawinsonde observation data and snowflake photographs collected at Gangneung-Wonju National University (GWNU) to analyze the thermodynamic structure of the lower-level atmosphere associated with the 29–30 January 2016. Figure 5a displays the results of time series of thermodynamic profiles at the GWNU site. The white flags, shading, and black solid lines represent the wind field (u–v), RH, and equivalent potential temperature, respectively. Analysis of the RH vertical profile revealed a well-developed, two-layered cloud structure with upper- and lower-level (≤ 2 km) clouds extending vertically. Above the lower cloud layer (2–3 km), an equivalent potential temperature inversion layer appeared, and a clear wind-directional shear was observed around 2-km altitude for the snowfall period (Fig. 5a). While the northerly or northeasterly wind was dominant in the lower level, the westerly wind was dominant in the upper level, which was also consistent with the radial velocity signals shown in Figs. 3c and d.

Figure 5b exhibits the 3-h accumulated snowfall and snow water equivalent over time, peaking at 6 cm and 8 mm, respectively, during the snowfall period together with the change in the 850 hPa temperature. Despite the surface temperature (Bukgangneung station) being above 0°C, the precipitation occurred exclusively as snowfall. From 0000

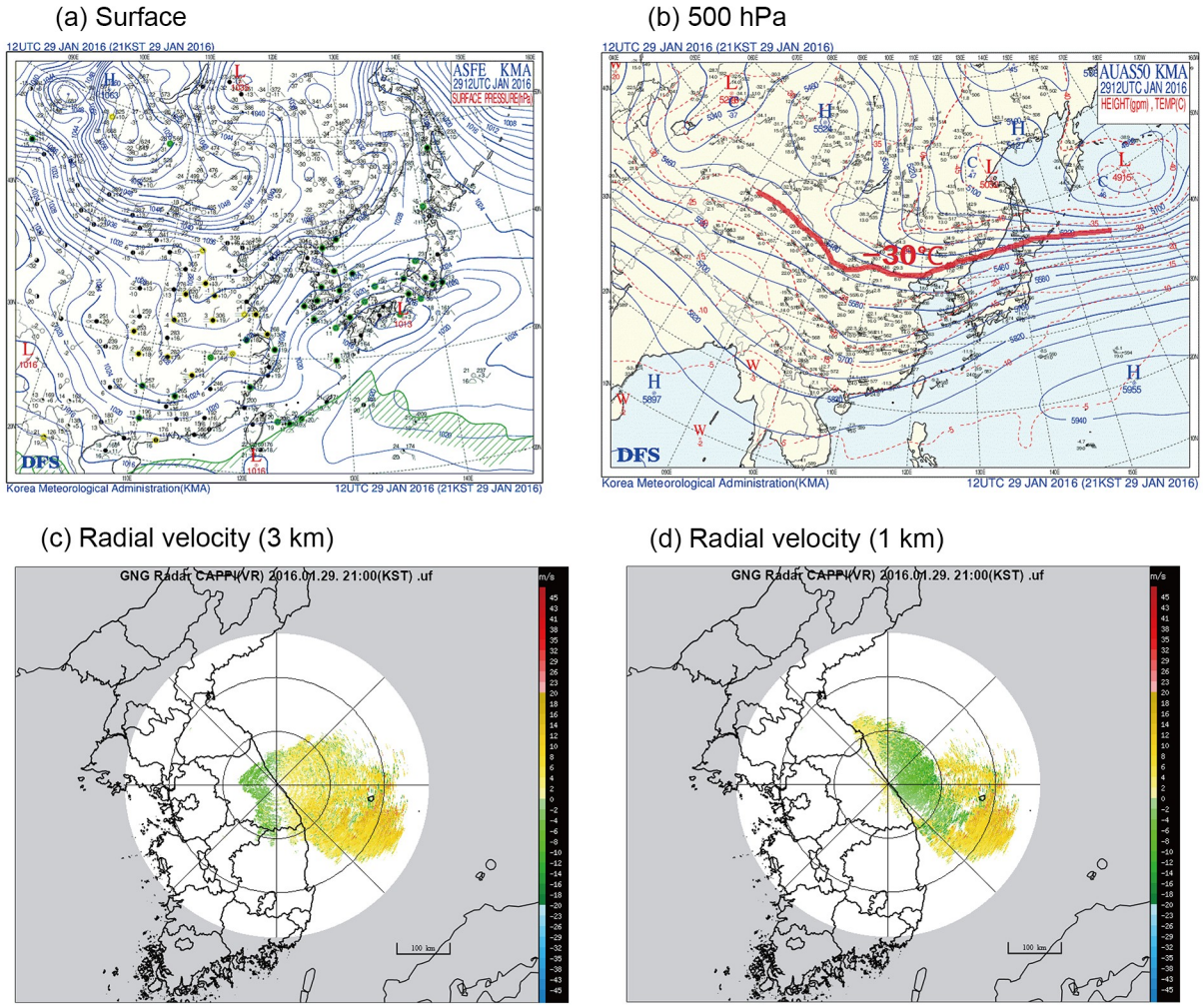

Fig. 3. (a) Surface weather chart, (b) upper-level (500-hPa) synoptic chart, and the radial velocity at (c) 3 km and (d) 1 km altitude from the S-band Doppler radar (CAPPI: constant altitude plan position indicator) at 1200 UTC 29 January 2016.

UTC onwards on 30 January, the northeasterly wind weakened, and the cloud layer stopped developing with snowfall ending at 0300 UTC (Figs. 5a and b). During this period, the 850 hPa temperature decreased to −8.5°C by 2100 UTC on 29 January and sharply rose again. Figure 5c shows the changes in the main snow crystal shape over time: during the middle part (described as Period I) of the snowfall episode, graupel-like snow crystals ($D \leqslant 3$ mm) were predominantly observed, which changed into dendrite-like particles in the later part (described as Period II) of the snowfall episode when the 850 hPa temperature decreased to −8.5°C. This implies that the shape of the snow crystals observed on the ground is primarily associated with the 850 hPa temperature change (Kim et al., 2018).

3.2.2. *Mountainous sites*

To gain insight into the cold cloud and snow crystal characteristics in the mountainous region, intensive observations of six-hourly rawinsonde and three-hourly snowflake photographing were also carried out at the Daegwallyeong (DAGW) site. Figure 6a shows time series of thermodynamic profiles using the rawinsonde data during the snowfall episode. Although upper-air soundings were performed at 6-h intervals, the results show a high coherence with GWNU's vertical profile (3-h intervals). We also found that two-layered clouds were observed along with the stronger inversion in equivalent potential temperature around 2–3 km and distinctive wind-directional shear. Northeasterly wind was dominant in the lower level, relative to westerly wind above 2-km altitude (sea level). Figure 6b presents temporal evolutions of precipitation and snowfall amount along with the 850-hPa temperature. The total accumulated precipitation and snowfall reached 2.8 mm and 5.5 cm, respectively, which means that the water equivalent ratio is relatively high at DAGW site. Both amounts at DAGW were much smaller than those at Bukgangneung.

Figure 6c shows the changes in the dominant snow crystals. In contrast to the GWNU site, the snow crystal habits observed at the DAGW site were largely needle or rimed needle. However, the graupel-like particles were frequently captured in the case of two-layered clouds, probably through the process of freezing of supercooled droplets on

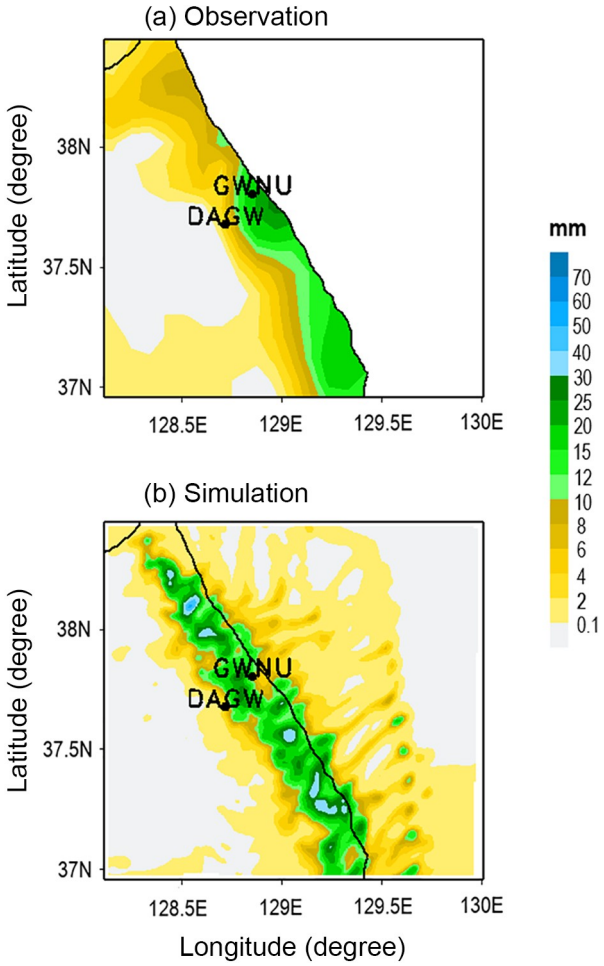

Fig. 4. Spatial distributions of total accumulated precipitation from 0000 UTC 29 January to 0600 UTC 30 January 2016 derived from (a) observations and (b) the CReSS simulation.

the ice particles. To identify the characteristics of cloud microphysics, we derived the particle size, cloud liquid water content, fall velocity, and any other relevant parameters from the MRR and PARSIVEL disdrometer at Alpensia (ALPN) located near the DAGW site. A number of MRR data had to be excluded from the dataset by manual quality checks due to dish heating problems, beam blockage issues, and so on (Maahn and Kollias, 2012; Schneebeli et al., 2013), as can be seen in Figs. 7a–c. Despite the limited data, there was some meaningful information. Average radar reflectivity and fall velocity of snow crystals were about 15 dBZ and 1.5 m s^{-1}, respectively (Figs. 7a and b). Interestingly, the high liquid water contents (0.4–1.0 g m^{-3}) around 0900 UTC 29 January (Fig. 7c) were correlated with the homogeneous graupel-like particles (Fig. 6c), which grow by the riming process of ice crystals with supercooled water droplets. Another thing to note is that droplets at the ground level had various sizes and numbers, including large diameter, with the broader range of 0.2–3.8 mm (Fig. 7d), when two-layered (thick) clouds developed vertically up to 5 km (around 1200 UTC 29 January), which is consistent with snow crystal images (mainly aggregates of needles) as shown in Fig. 6c. The homogeneous habits, such as needle or graupel with small size (D < 3 mm), were observed after 1800 UTC 29 January, when the 850-hPa temperature dropped to −8.5°C and the growth of snow crystals and vertical development of clouds began to weaken (Figs. 6c and 7d).

3.3. *Sensitivity experiments*

3.3.1. *CTRL experiment*

The cloud-resolving simulations were carried out to identify the characteristics of cold clouds and snow crystals based on the observations. First, we evaluated the model performance by comparing the accumulated precipitation distribution between the CReSS model and the observations (Figs. 4a and b). The observed precipitation was interpolated using the dataset from the 107 automatic weather stations located in the analysis domain. Although the control (CTRL) simulation overestimated the precipitation in some parts of the northern Yeongdong region, the overall horizontal distributions of precipitation coincided fairly well with those of the observed precipitation (with precipitation concentrated along the Yeongdong coast). Figure 8a presents time series of vertical profiles derived from the CReSS simulation for the CTRL run. The comparison of the simulated and observed results at the GWNU site identified that the CReSS model represented the cloud characteristics well, such as the height of the lower-level cloud and the two-layered cloud structure (Figs. 5a and 8a). Wind-directional shear and the inversion of the equivalent potential temperature above the lower cloud layer were also in good agreement with the observed features as shown in Fig. 5a. In the CTRL experiment at GWNU grid point, rain was simulated most frequently during the analysis period, generally resulting in underestimating the snow amount compared with the observations. However, both the simulation and observation results agreed well with each other in the snowfall period (1200–1800 UTC 29 January), when graupel habits of snow crystals were dominant (Figs. 5c and 9a).

Figure 10a displays time series of thermodynamic profiles from the CTRL simulation at the DAGW grid point. The simulation results also show a high coherence with DAGW's vertical profiles obtained from upper-air observations at 772 m above sea level (Figs. 6a and 10a). The RH profiles reveal that the two-layered cloud structure was well simulated. The wind-directional shear and distinctive inversion in equivalent potential temperature around 2–3 km match well with the observation. Figure 11a shows the proportion of 3-h accumulated precipitation by each hydrometeor component derived from the CTRL simulation at DAGW. Total simulated precipitation (3 mm) was similar to DAGW's observation (Fig. 6b) in terms of amount (2.8 mm) and peak time (1500 UTC 29 January). In comparison with the CTRL experiment for GWNU, decreasing (about 69%) total precipitation and increasing proportions of simulated snow particles were clearly demonstrated in the CTRL experiment for DAGW (Table 3). The following three sensitivity experi-

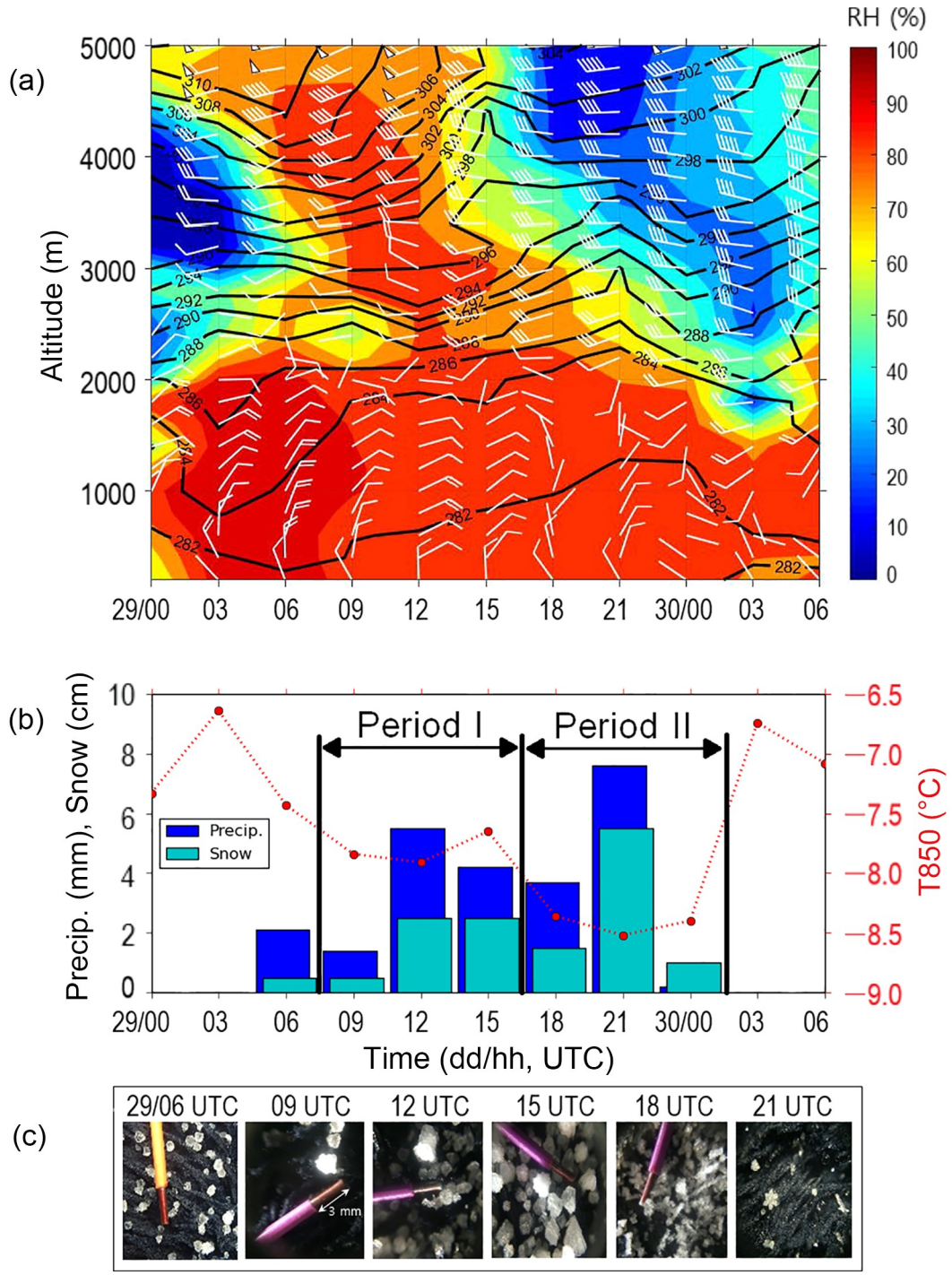

Fig. 5. Time series of (a) thermodynamic profiles, (b) snow and precipitation amounts along with the 850-hPa temperature, and (c) the main snow crystal habits on 29–30 January 2016 at the GWNU site. The white flags, shading, and black solid lines in (a) denote the *u*–*v* wind (units: m s^{-1}), relative humidity (units: %), and equivalent potential temperature (units: K), respectively.

ments were performed based on the reliable CTRL experiment results.

3.3.2. *TEMP experiment*

First, the temperature reduction (TEMP) experiment was conducted to investigate the change in precipitation particle characteristics when the lower level (below the 850 hPa level, where there is always a cloud layer) is cooled by 3°C. The results are presented in Fig. 8b. The low-level cloud layer, which developed to over 2 km in the CTRL experiment, became thinner (less than 1.5 km), and cloud dissipation even occurred in some parts of the simulation segment (0600–1200 UTC 29 January), presumably attributable to the weak northeasterly winds simulated at altitudes

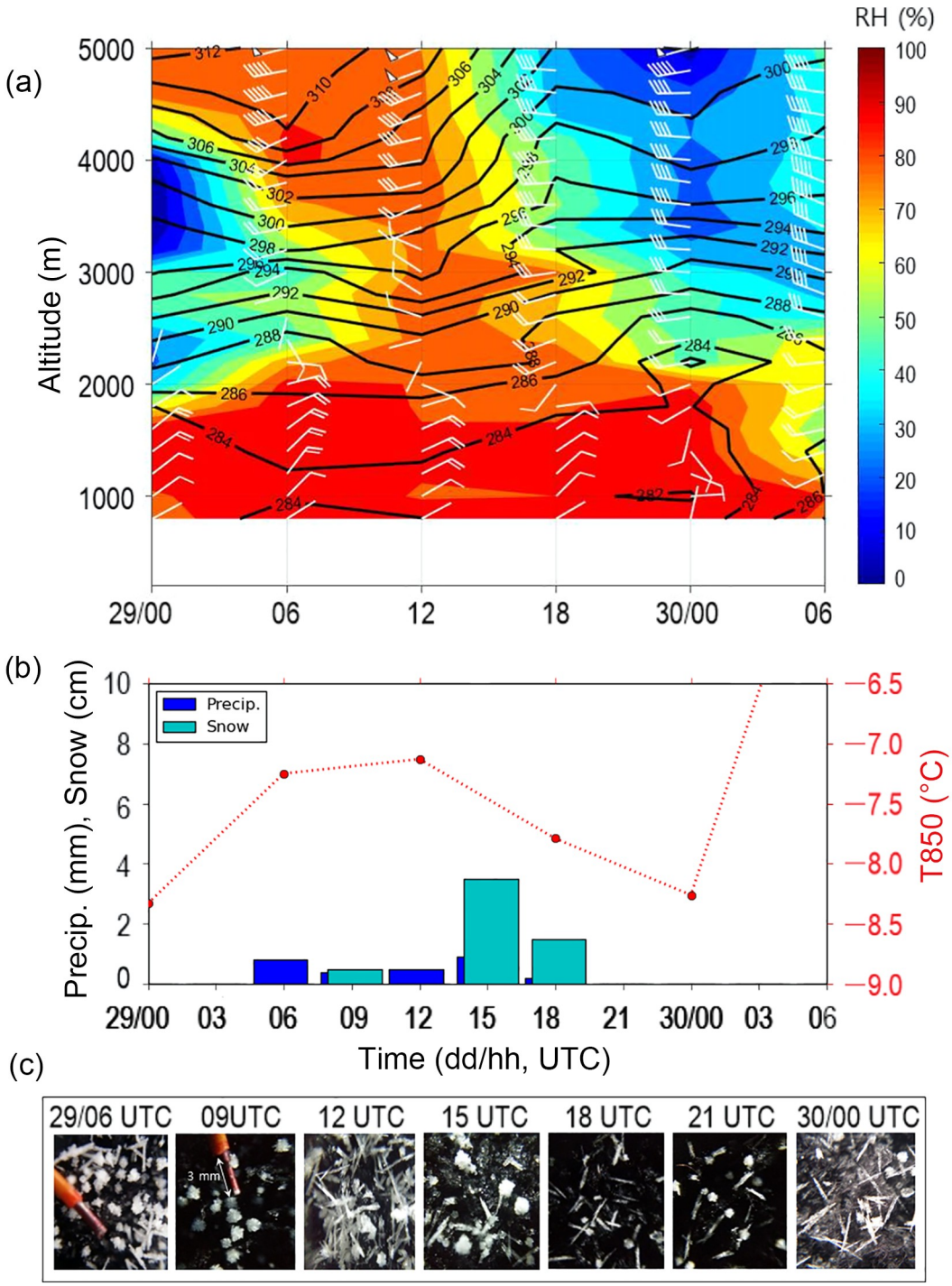

Fig. 6. As in Fig. 5 except for the DAGW site.

of 500 m or less. The decrease in the planetary boundary layer height induced by the decreasing surface temperature is also assumed to be responsible for the decreases in cloud thickness and precipitation. However, the inversion layer of the equivalent potential temperature above the low-level cloud layer and the wind-directional shear exhibited between the upper and lower levels were still in good agreement with the CTRL experiment results. Next, we compared the characteristics of the 3-h accumulated precipitation types simulated in the CTRL and TEMP experiments (Figs. 9a and 9b). Although the total accumulated precipitation decreased by 87% in the TEMP experiment compared with that in the CTRL experiment, the changing precipitation type trend was identified (Table 3).

For a more detailed comparison of the time-dependent changes in the precipitation particle characteristics, we divided the middle and latter parts of the CTRL and TEMP experiments into Period I (0900–1500 UTC 29 January) and

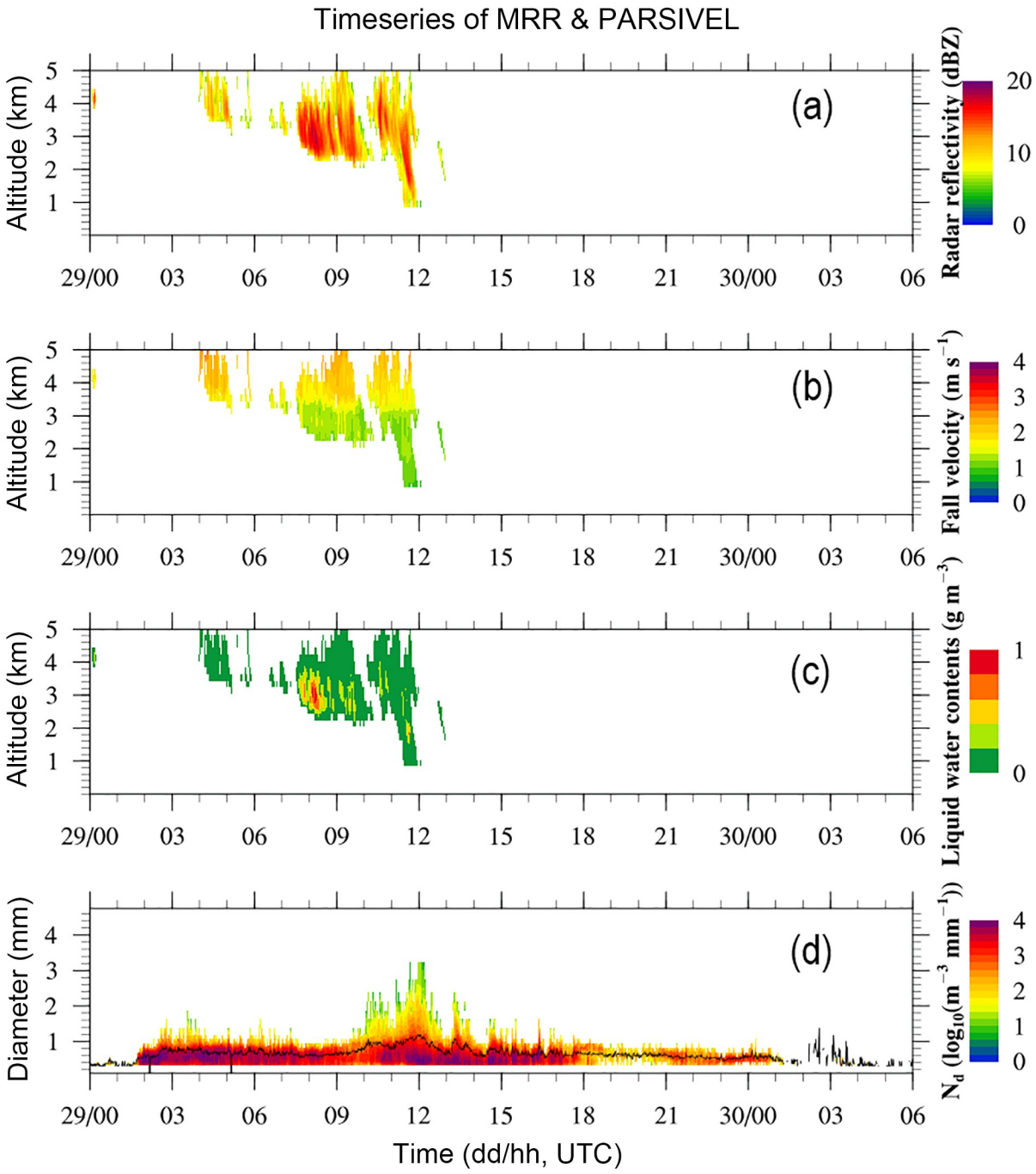

Fig. 7. Time series of (a) radar reflectivity, (b) fall velocity, (c) cloud liquid water content retrieved from MRR, and (d) mean diameter and number concentration of droplets from the PARSIVEL disdrometer at the ALPN site.

Period II (1800 UTC 29 January to 0000 UTC 30 January) and analyzed the proportions of rain, graupel, and snow particles. The rain amount, which accounted for 47%–67% of the precipitation in both periods in the CTRL experiment, was reduced to less than 10% in the TEMP experiment. However, compared with the CTRL experiment, increasing proportions of graupel and snow particles were clearly demonstrated in the TEMP experiment (a 2.3 times increase of the graupel particle proportion in Period I and a 22.5 times increase of the snow particle proportion in Period II). From these results, it can be inferred that when low-level temperature decreases, the overall precipitation decreases; however, rain particles turn into riming- or aggregation-like (graupel) particles in Period I, and the proportion of dendrite-like (snow) particles increases as the temperature further decreases in Period II. This also implies that the precipitation particle characteristics in the Yeongdong coastal region are primarily determined by the low-level (below the 850 hPa level) temperature.

At the mountainous site, the easterly-induced thin cloud

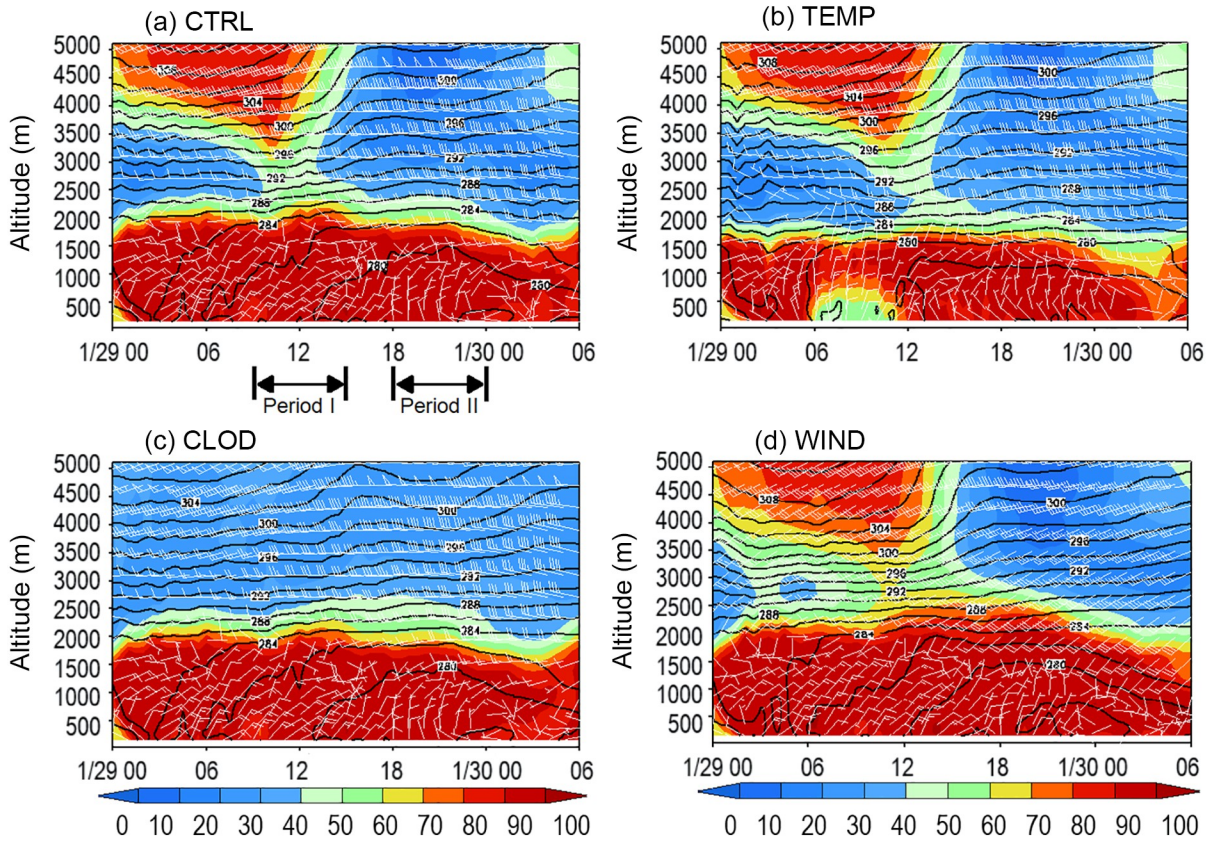

Fig. 8. As in Fig. 5a except for the CReSS simulations from 0000 UTC 29 January 2016 to 0600 UTC 30 January 2016 for the (a) CTRL, (b) TEMP, (c) CLOD, and (d) WIND experiments at the GWNU grid point.

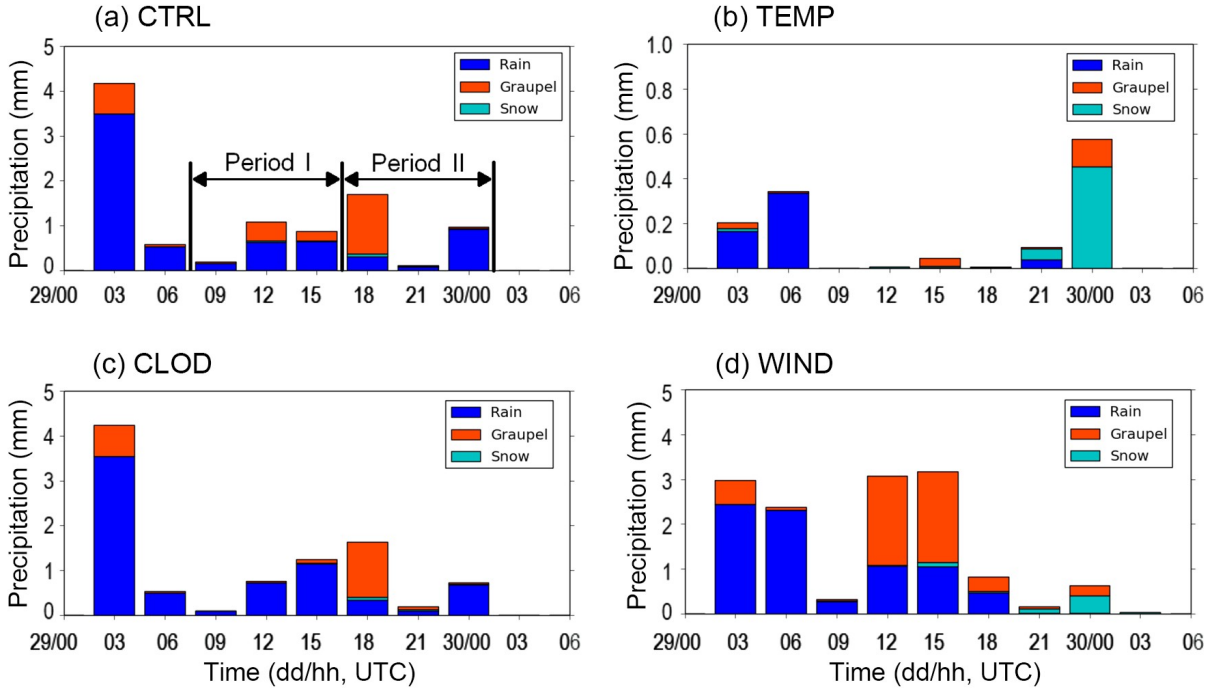

Fig. 9. Time series of 3-h accumulated precipitation of rain, graupel, and snow derived from CReSS simulations for the (a) CTRL, (b) TEMP, (c) CLOD, and (d) WIND experiments at the GWNU grid point. The y-axis is the same scale except for the TEMP experiment.

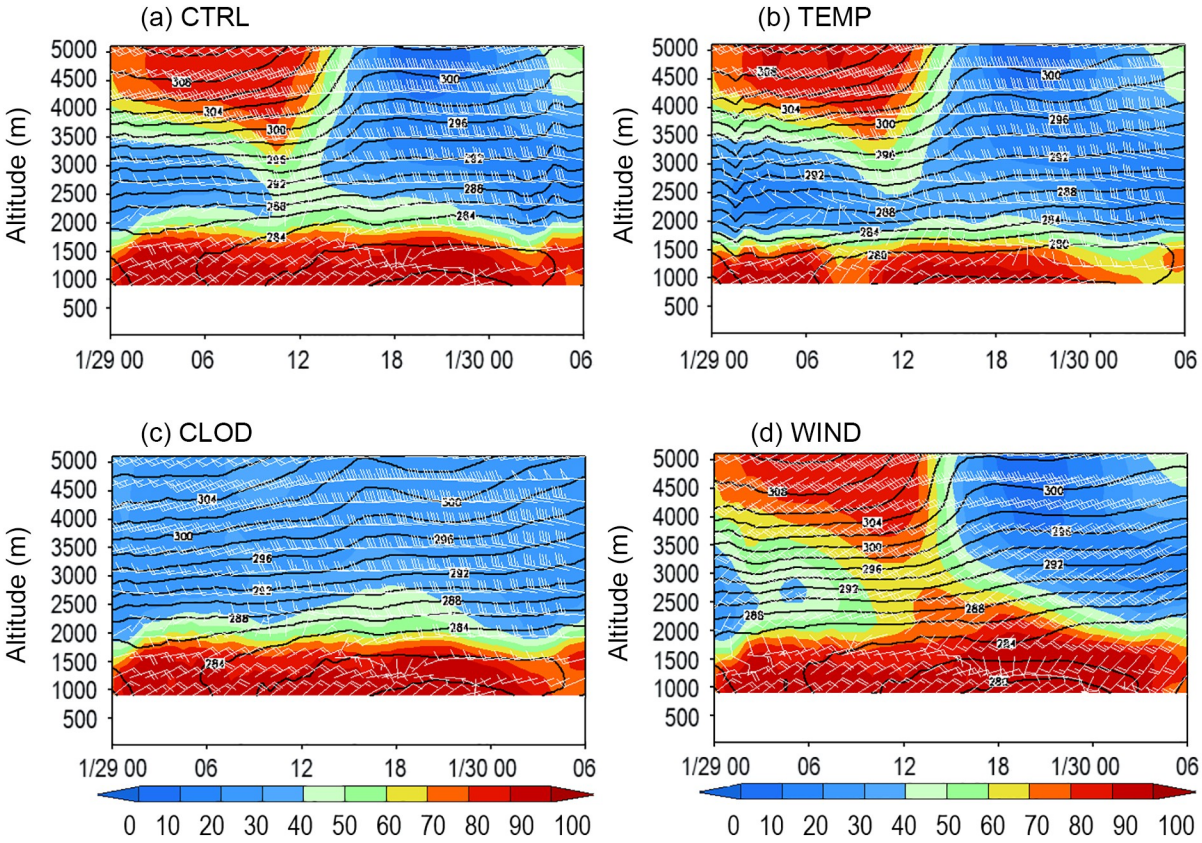

Fig. 10. As in Fig. 8 except for the CReSS simulations from 0000 UTC 29 January 2016 to 0600 UTC 30 January 2016 at the DAGW grid point.

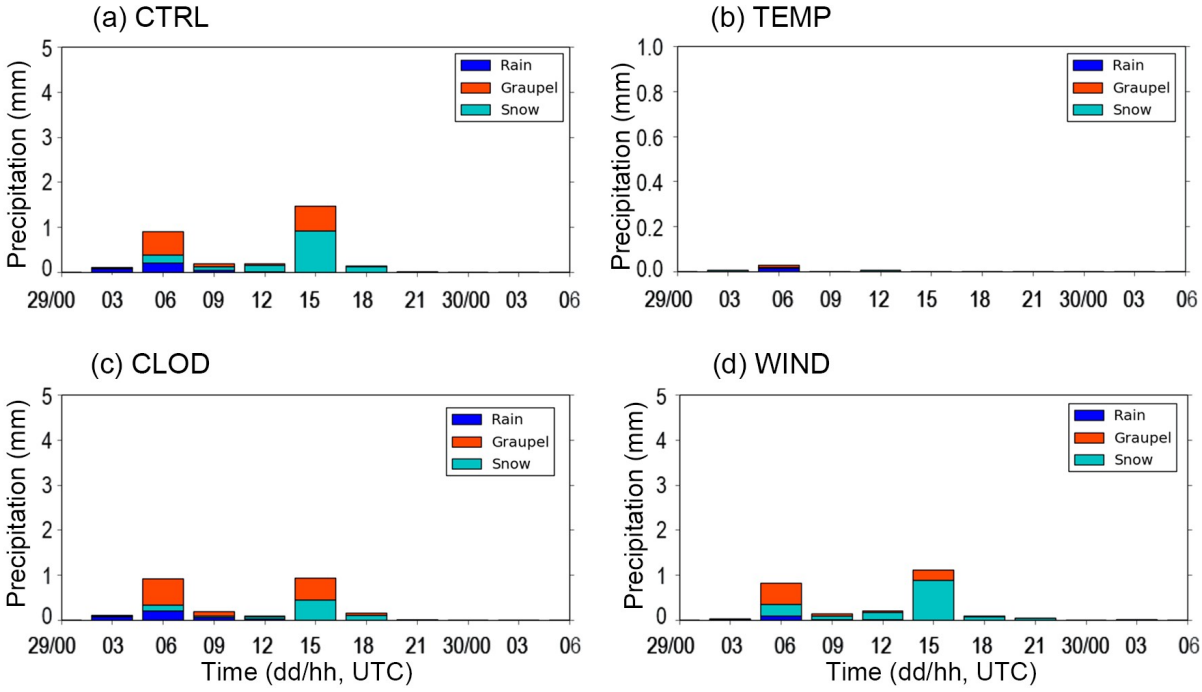

Fig. 11. As in Fig. 9 except for the DAGW grid point.

system was reflected well at the DAGW grid point, where there was little precipitation (Table 3). It seems to be associated with the retreat of convergence and the precipitation zone to the East Sea.

Table 3. Summary of precipitation for different experiments. Units: mm.

Experiments	CTRL EXP		TEMP EXP		CLOD EXP		WIND EXP	
GWNU	Total	9.7	ΔP^a	(−) 8.4	ΔP	(−) 0.2	ΔP	(+) 3.9
	Rain	6.8	ΔR^a	(−) 6.2	ΔR	(+) 0.4	ΔR	(+) 0.9
	Graupel	2.8	ΔG^a	(−) 2.6	ΔG	(−) 0.6	ΔG	(+) 2.4
	Snow	0.1	ΔS^a	(+) 0.4	ΔS	0.0	ΔS	(+) 0.6
DAGW	Total	3.0	ΔP	(−) 3.0	ΔP	(−) 0.6	ΔP	(−) 0.5
	Rain	0.3	ΔR	(−) 0.3	ΔR	(+) 0.1	ΔR	(−) 0.1
	Graupel	1.2	ΔG	(−) 1.2	ΔG	0.0	ΔG	(−) 0.4
	Snow	1.5	ΔS	(−) 1.5	ΔS	(−) 0.7	ΔS	0.0

Note: ΔP^a, ΔR^a, ΔG^a and ΔS^a denote the differences in total precipitation, rain, graupel and snow, respectively, between each experiment and CTRL.

3.3.3. *CLOD experiment*

Secondly, in order to investigate the effects of the two-layered cloud system on snowfall in the Yeongdong region, we performed a single-layered cloud (CLOD) experiment by changing the initial and boundary conditions of the CReSS model from a two-layered cloud system to a single-layered cloud system. The results of the CLOD experiment for the GWNU site are presented in Figs. 8c and 9c. The original two-layered cloud system was well simulated as a single-layered cloud system. While no significant changes were observed when compared with the CTRL experiment in terms of the overall precipitation amount, the change in precipitation type from rain (CLOD) to graupel (CTRL) in Period I, during which the distance between the upper and lower layers of the cloud was smallest, was manifested (Figs. 9a and c). In the CLOD experiment, the proportion of graupel particles decreased by approximately 25%, and the proportion of rain particles increased by approximately 27% in Period I, whereas similar proportions of graupel and rain for both experiments were analyzed in Period II, with small differences of 2.2% and 3.6%, respectively. The increase in the proportion of graupel on the surface in the CTRL experiment may be interpreted as the result of the riming of ice particles in the upper-layer cloud to supercooled liquid water while falling. However, the difference in the total precipitation amount between CLOD and CTRL was not significant enough to explain the effect of the two-layered cloud system (Table 3).

To further investigate the impacts of the seeder–feeder process in the experiment between CTRL and CLOD, we examined the vertical distribution of mixing ratios of hydrometeors between the cloud layers in the CTRL experiment. Figure 12 shows the vertical profiles of water vapor (shading), snow (grey line), ice (yellow line), and graupel (red line) derived from the CReSS simulations for the CTRL and CLOD experiments at the GWNU grid point. In comparing the vertical distributions of both experiments, the mixing ratios of three hydrometeors were partially increased in the CTRL experiment during Period I (Fig. 12a). The amounts of the three mixing ratios (< 0.05 g kg^{-1}) were not enough to be sensitive to a change in the seeder–feeder effect, which corresponds well with the small difference in total

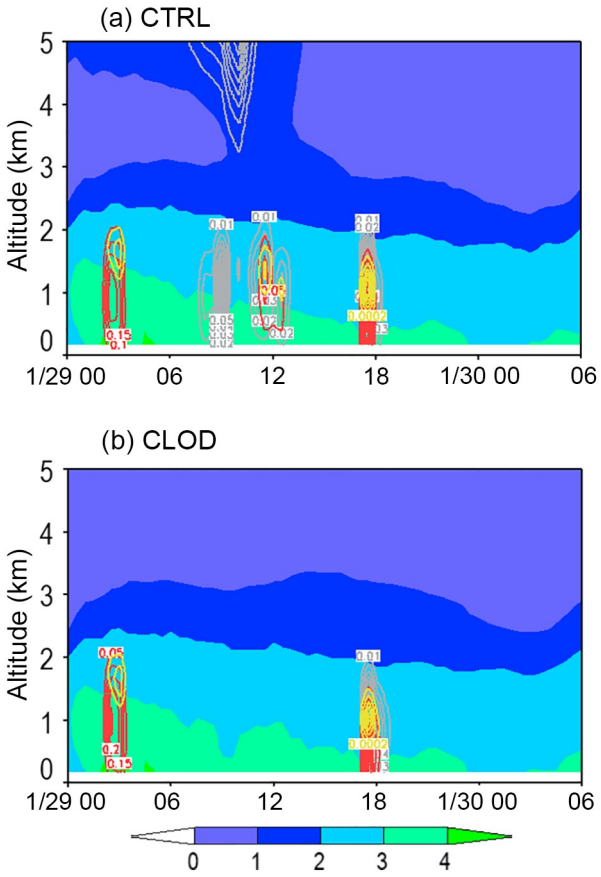

Fig. 12. Vertical profiles of mixing ratio (units: g kg^{-1}) of water vapor (shading), snow (gray lines), ice (yellow lines), and graupel (red lines) derived from CReSS simulations from 0000 UTC 29 January 2016 to 0600 UTC 30 January 2016 for the (a) CTRL and (b) CLOD experiments at the GWNU grid point.

(i.e., all hydrometeor categories) precipitation amount, as shown in Figs. 9a and c. Rather, it may be attributed to a weakened seeder–feeder process as a result of the dry surrounding environments (altitude: 2–3.5 km) due to the small amounts (1–2 g kg^{-1}) of the water vapor mixing ratio.

On the other hand, the cloud morphology of the DAGW site was similar to that of the GWNU site in terms of cloud height and dissipation of upper-level cloud (Fig. 10c). Compared to CTRL's results for DAGW, the total precipita-

tion amount was reduced to less than 3 mm (Figs. 11a and c). Table 3 summarizes each particle for the CTRL and CLOD experiments at the DAGW site. Interestingly, CLOD's results show that the amount of graupel was unchanged, but that of snow was decreased by 0.7 mm (about 47%), against CTRL. Certainly, the absence of the snow mixing ratio in the upper cloud layer may have contributed to the significant decrease in snow particles at DAGW for the CLOD experiment (Fig. 12).

3.3.4. *WIND experiment*

One of the most remarkable characteristics of snowfall events in the Yeongdong region is the wind-directional shear above the cloud layer (Fig. 5a). To investigate the effect of this wind-directional shear on the snow crystals and snowfall characteristics, we conducted the WIND experiment with the wind-directional shear effect weakened. The setup of the WIND experiment is explained in detail in section 2. Figure 8d shows time series of thermodynamic profiles from the CReSS simulation for the WIND experiment at the GWNU grid point. From the results, it can be seen that the characteristics of the two-layered cloud structure exhibited a more coupled behavior in the WIND experiment, and the characteristics of the low-level cloud developing up to a much higher altitude (2.5 km) were observed throughout the simulation (Fig. 8d). In addition, southwesterly wind was dominant above 2.5 km up to a higher altitude. That is, the effect of the wind-directional shear between the upper and lower levels, which represents the typical vertical profiles in the Yeongdong region, was reduced in the WIND experiment, and the wind field at the altitude of the lower-level cloud (~ 2 km) and above is thought to have facilitated the development of the cloud vertically.

The analysis results of the precipitation characteristics simulated in the WIND experiment at the GWNU grid point are presented in Fig. 9d. A comparison of the total precipitation amount revealed more than 1.4 times the amount of precipitation in the WIND experiment (13.6 mm) versus the CTRL experiment (Table 3). Rain particles, which accounted for the largest proportion (67% in Period I) of precipitation in the CTRL experiment, decreased in the WIND experiment, with the proportions of graupel in Period I and snow in Period II increasing (Figs. 9a and d). In particular, graupel particles accounted for the highest proportion (~62%) in Period I, during which precipitation was most intense in the WIND experiment (Fig. 9d). This may be ascribed to the equivalent potential temperature (282–284 K) along with the southwesterly wind being slightly higher in the WIND experiment than in the CTRL experiment (Fig. 8d), which increased the amount of liquid water, and the riming process induced by the vertical development of the cloud is assumed to have accelerated the generation of graupel particles (Fig. 9d).

At the DAGW grid point, vertical development of low-level cloud and the coupled feature between upper and lower clouds are also represented in the simulation of thermodynamic profiles in Fig. 10d. Here, we found that the wind-directional shear was reduced, whereas the large-scale dynamics of the upper level were still preserved. Interestingly, the smoothing wind field in the vicinity of the shear layer altered the cloud structure to facilitate a much deeper cloud system, but the accumulated precipitation (2.5 mm) decreased compared to the CTRL experiment (Table 3). The amount of snow in the WIND experiment did not change, but that of graupel decreased by 0.4 mm for the analysis period. This might be associated with the retreat of clouds and the precipitation zone to the coast (Figs. 13b and d), similarly to the TEMP experiment, probably induced by the weakening of wind-directional shear, which eventually results in the decrease in total precipitation at DAGW.

4. Summary and discussion

To investigate the characteristics of cold clouds and snow crystals in both the coastal and mountainous regions of Yeongdong, we selected a heavy snowfall episode that occurred on 29–30 January 2016. We analyzed the results of intensive observations using rawinsonde soundings and snowflake photographs with high temporal resolution. We also conducted sensitivity experiments using a CReSS model to identify the effects of critical meteorological factors on precipitation characteristics specific to the Yeongdong region.

The analysis of atmospheric profiles using intensive observational data from coastal (GWNU) and mountainous (DAGW) sites revealed a well-developed, two-layered cloud structure along with an inversion layer of the equivalent potential temperature above the low-level cloud. Furthermore, wind-directional shear between the upper and lower levels was clearly exhibited, with the northerly or northeasterly wind dominant in the lower level ($\leqslant$ ~2 km) and the westerly wind dominant in the upper level ($>$ 2 km) during the snowfall period. The main snow crystals changed from riming particles in the middle part (Period I) of the snowfall event to dendrite particles in the latter part (Period II), as the 850-hPa temperature decreased from −7.5°C to approximately −8.5°C at the GWNU site, whereas, the snow crystal habits observed at the DAGW site were largely needle or rimed needle for the whole period. From the MRR and PARSIVEL observations, the high liquid water contents around 0900 UTC 29 January were correlated with the homogeneous graupel-like particles, and droplets with various sizes and numbers (around 1200 UTC) were consistent with snow crystal images (aggregates of needles) obtained from snowflake photography (DAGW).

The simulated and observed accumulated precipitation distributions showed fairly good agreement, with the cloud characteristics, including cloud height, the two-layered cloud structure, and thermodynamic profiles (wind-directional shear and the inversion of equivalent potential temperature), well simulated by the CReSS model. We attempted to evaluate the sensitivity of this snow storm to 850-hPa temperature, the seeder–feeder mechanism, and wind-directional shear. Three sensitivity experiments were performed with

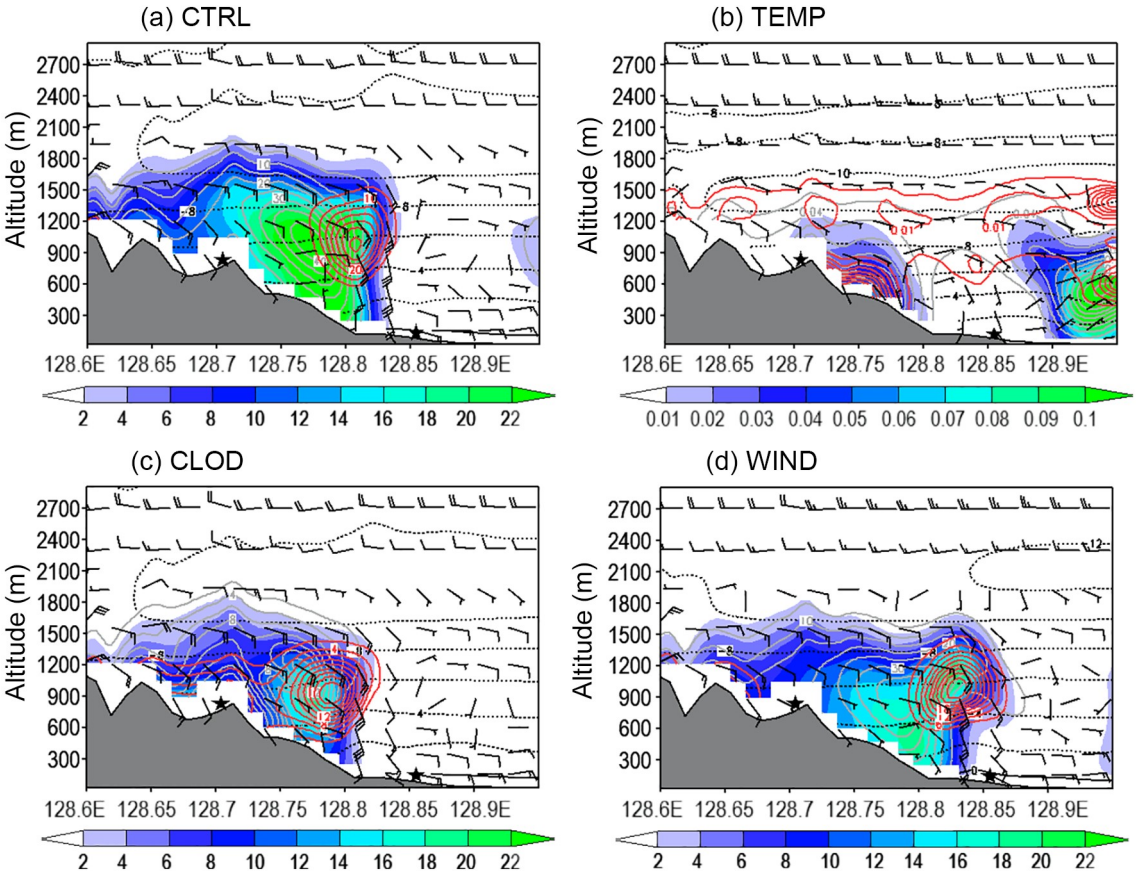

Fig. 13. Vertical cross sections of the number concentrations of graupel (shading), snow (gray lines), and ice (red lines) along with the fields of u–w wind (flags) and air temperature (dashed lines) for the (a) CTRL, (b) TEMP, (c) CLOD, and (d) WIND experiments at 1200 UTC 29 January 2016. The star symbols denote the locations of the DAGW (left) and GWNU (right) sites.

the following results.

First, in the TEMP experiment, in which the lower level (≤ 850 hPa) was cooled by 3°C from the CTRL experiment, the low-level cloud thickness was reduced to less than 1.5 km, and the overall accumulated precipitation was decreased by 87%. It was found that the upslope winds and vertical development of clouds (number concentrations) were weakened compared to the CTRL experiment, as shown in Figs. 13a and b, which eventually resulted in the decrease in precipitation (especially at the mountainous site). However, the importance of the temperature in the low-level layer could be identified from the increase in the proportions of graupel particles (~2.3 times greater than in CTRL) in Period I and snow particles (~22.5 times greater than in CTRL) in Period II at the GWNU grid point.

Secondly, in the CLOD experiment, in which the initial boundary conditions were changed from a two-layered to single-layered cloud system in order to investigate the effects of the two-layered cloud structure on the snowfall episode in the Yeongdong region, no significant differences were observed between the CTRL and CLOD experiments in the overall precipitation amount. However, the increase in the graupel proportion in the CTRL experiment (two-layered) may be interpreted as being the result of the ice-phase particles from the upper-layer cloud riming to supercooled liquid water while falling. The characteristics in the CTRL experiment discussed above were consistent with the increase in the number concentration of graupel, especially for the coastal region (Figs. 13a and c).

Lastly, in the WIND experiment, in which the effect of the wind-directional shear above the lower cloud layer was weakened, the characteristics of the two-layered cloud structure exhibited in CTRL were more coupled, and the low-level cloud was observed to develop up to a much higher altitude (2.5 km). The precipitation at GWNU was increased by 1.4 times greater than the CTRL experiment, with graupel particles accounting for the highest proportion (~62%) in Period I, during which the precipitation rate increased. At DAGW, the accumulated precipitation (2.5 mm) decreased compared to the CTRL experiment, which can be interpreted as a result of the shift in convergence and the precipitation zone closer to the Yeongdong coastal area induced by weakening of wind-directional shear (Figs. 13a and d).

Various sensitivity experiments based on cloud-resolving modeling led to verification that precipitation particle characteristics are primarily determined by the temperature in the lower levels and that the meteorological conditions in the Yeongdong region, characterized by a dry condition

between cloud layers, are not favorable for the seeder–feeder mechanism. Furthermore, the experimental results imply that the vertical wind-directional shear could change the location of precipitation in the Yeongdong region, such as retreating to the coast. Although this research has only focused on one snowfall episode, the current results could be used as a foundation for improving the predictability of snowfall in the Yeongdong region. However, to improve the prediction accuracy of the snowfall type, it is necessary to consider not only vertical thermodynamic profiles but also complex processes such as turbulence within cloud layers and the vertical velocity (Zerr, 1997; Pinsky and Khain, 1998). To this end, a more detailed and in-depth understanding of the microphysical characteristics of clouds is required with the aid of in-situ or remote sensing observations, such as aircraft observations and multi-angle snowflake cameras.

Acknowledgements. This work was funded by the Korea Meteorological Administration Research and Development Program "Development and Application of Monitoring, Analysis and Prediction Technology for High Impact Weathers" (Grant No. KMA2018–00123), and partly supported by the Basic Science Research Program through the National Research Foundation of Korea funded by the Ministry of Education (Grant No. 2015R1D1A1A0105 7211).

REFERENCES

Bergeron, T., 1950: Über der mechanismus der ausgiebigen Niederschläge. *Ber. Deut. Wetterd.*, **12**, 225–232.

Cooper, S. J., N. B. Wood, and T. S. L'Ecuyer, 2017: A variational technique to estimate snowfall rate from coincident radar, snowflake, and fall-speed observations. *Atmospheric Measurement Techniques*, **10**, 2557–2571, https://doi.org/10.5194/amt-10-2557-2017.

Grazioli, J., G. Lloyd, L. Panziera, C. R. Hoyle, P. J. Connolly, J. Henneberger, and A. Berne, 2015: Polarimetric radar and in situ observations of riming and snowfall microphysics during CLACE 2014. *Atmospheric Chemistry and Physics*, **15**, 13 787–13 802, https://doi.org/10.5194/acp-15-13787-2015.

Houze, R. A., and S. Medina, 2005: Turbulence as a mechanism for orographic precipitation enhancement. *J. Atmos. Sci.*, **62**, 3599–3623, https://doi.org/10.1175/JAS3555.1.

Houze, R. A., S. A. Rutledge, T. J. Matejka, and P. V. Hobbs, 1981: The mesoscale and microscale structure and organization of clouds and precipitation in midlatitude cyclones. *III: Air motions and precipitation growth in a warm-frontal rainband. J. Atmos. Sci.*, **38**, 639–649, https://doi.org/10.1175/1520-0469(1981)038<0639:TMAMSA>2.0.CO;2.

Kim, Y. J., B. G. Kim, J. K. Shim, and B. C. Choi, 2018: Observation and numerical simulation of cold clouds and snow particles in the Yeongdong region. *Asia-Pacific Journal of Atmospheric Sciences*, **54**, 499–510, https://doi.org/10.1007/s13143-018-0055-6.

Ko, A. R., B. G. Kim, S. H. Eun, Y. S. Park, and B. C. Choi, 2016: Analysis of the relationship of water vapor with precipitation for the winter ESSAY (Experiment on Snow Storms at Yeongdong) period. *Atmosphere*, **26**(1), 19–33, https://doi.org/10.14191/Atmos.2016.26.1.019.

Kwon, T. Y., and Coauthors, 2006: Development of Yeongdong heavy snowfall forecast supporting system. *Atmosphere*, **16**(3), 247–257.

Lee, K. O., S. Shimizu, M. Maki, C. H. You, H. Uyeda, and D. I. Lee, 2010: Enhancement mechanism of the 30 June 2006 precipitation system observed over the northwestern slope of Mt. *Halla, Jeju Island, Korea. Atmospheric Research*, **97**, 343–358, https://doi.org/10.1016/j.atmosres.2010.04.008.

Lin, Y. L., L. J. Donner, and B. A. Colle, 2011: Parameterization of riming intensity and its impact on ice fall speed using ARM data. *Mon. Wea. Rev.*, **139**, 1036–1047, https://doi.org/10.1175/2010MWR3299.1.

Liu, G. S., 2008: A database of microwave single-scattering properties for nonspherical ice particles. *Bull. Amer. Meteor. Soc.*, **89**, 1563–1570, https://doi.org/10.1175/2008BAMS2486.1.

Maahn, M., and P. Kollias, 2012: Improved micro rain radar snow measurements using Doppler spectra post-processing. *Atmospheric Measurement Techniques*, **5**, 2661–2673, https://doi.org/10.5194/amt-5-2661-2012.

Medina, S., and R. A. Houze Jr, 2015: Small-scale precipitation elements in midlatitude cyclones crossing the California Sierra Nevada. *Mon. Wea. Rev.*, **143**, 2842–2870, https://doi.org/10.1175/MWR-D-14-00124.1.

Ministry of the Interior and Safety, 2016: *2016 Statistical Yearbook of Natural Disasters*. Ministry of the Interior and Safety, Korea, 927 pp. [Available online from https://www.mois.go.kr/frt/bbs/type001/commonSelectBoardArticle.do?bbsId=BBSMSTR_000000000014&nttId59551] (in Korean)

Molthan, A. L., W. A. Petersen, S. W. Nesbitt, and D. Hudak, 2010: Evaluating the snow crystal size distribution and density assumptions within a single-moment microphysics scheme. *Mon. Wea. Rev.*, **138**, 4254–4267, https://doi.org/10.1175/2010MWR3485.1.

Murakami, M., 1990: Numerical modeling of dynamical and microphysical evolution of an isolated convective cloud-the 19 July 1981 CCOPE cloud. *J. Meteor. Soc. Japan*, **68**, 107–128, https://doi.org/10.2151/jmsj1965.68.2_107.

Murakami, M., T. L. Clark, and W. D. Hall, 1994: Numerical simulation of convective snow clouds over the sea of Japan. *J. Meteor. Soc. Japan*, **72**, 43–62, https://doi.org/10.2151/jmsj1965.72.1_43.

Nam, H. G., B. G. Kim, S. O. Han, C. K. Lee, and S. S. Lee, 2014: Characteristics of easterly-induced snowfall in Yeongdong and its relationship to air-sea temperature difference. *Asia-Pacific Journal of Atmospheric Sciences*, **50**, 541–552, https://doi.org/10.1007/s13143-014-0044-3.

Oue, M., M. Galletti, J. Verlinde, A. Ryzhkov, and Y. H. Lu, 2016: Use of X-band differential reflectivity measurements to study shallow arctic mixed-phase clouds. *J. Appl. Meteorol. Climatol.*, **55**, 403–424, https://doi.org/10.1175/JAMC-D-15-0168.1.

Pinsky, M. B., and A. P. Khain, 1998: Some effects of cloud turbulence on water-ice and ice-ice collisions. *Atmospheric Research*, **47–48**, 69–86, https://doi.org/10.1016/S0169-8095(98)00041-6.

Schneebeli, M., N. Dawes, M. Lehning, and A. Berne, 2013: High-resolution vertical profiles of X-band polarimetric radar observables during snowfall in the Swiss Alps. *J. Appl. Meteorol. Climatol.*, **52**, 378–394, https://doi.org/10.1175/JAMC-D-12-015.1.

Seo, W. S., and Coauthors, 2015: Study on characteristics of snow-

fall and snow crystal habits in the ESSAY (Experiment on Snow Storms at Yeongdong) campaign in 2014. *Atmosphere*, **25**(2), 261–270, https://doi.org/10.14191/Atmos.2015.25.2.261.

Thériault, J. M., and Coauthors, 2012: A case study of processes impacting precipitation phase and intensity during the Vancouver 2010 Winter Olympics. *Wea. Forecasting*, **27**, 1301–1325, https://doi.org/10.1175/WAF-D-11-00114.1.

Thériault, J. M., K. L. Rasmussen, T. Fisico, R. E. Stewart, P. Joe, I. Gultepe, M. Clément, and G. A. Isaac, 2014: Weather observations on Whistler mountain during five storms. *Pure Appl. Geophys.*, **171**, 129–155, https://doi.org/10.1007/s00024-012-0590-5.

Tsuboki, K., and A. Sakakibara, 2001: CReSS user's guide 2nd edition, 210 pp.

Tsuboki, K., and A. Sakakibara, 2002: Large-scale parallel computing of cloud resolving storm simulator. *Proc. 4th Int. Symp. on High Performance Computing*, Kansai Science City, Japan: Springer, 243–259, https://doi.org/10.1007/3-540-47847-7_21.

Tsuboki, K., and A. Sakakibara, 2007: Numerical prediction of high-impact weather systems. *Proc. 17th IHP Training Course (Int. Hydrological Program)*, Nagoya, Japan, International Hydrological Programme.

WMO, 2008: Guide to meteorological instruments and methods of observation. (CIMO Guide) 8th Edition: Part II. Observing systems, Chapter 7. Radar measurements, WMO-No. 8, World Meteorological Organization, Geneva, 680–750.

Zerr, R. J., 1997: Freezing rain: An observational and theoretical study. *J. Appl. Meteorol.*, **36**, 1647–1661, https://doi.org/10.1175/1520-0450(1997)036<1647:FRAOAT>2.0.CO;2.